HHS Public Access

Author manuscript

Glia. Author manuscript; available in PMC 2024 June 01.

Published in final edited form as:

Glia. 2023 June ; 71(6): 1466–1480. doi:10.1002/glia.24351.

Modulation of Schwann Cell Homeostasis by the BAP1 Deubiquitinase

Phu Duong[1,2], **Raghu Ramesh**[1,3], **Andrew Schneider**[1], **Seongsik Won**[1], **Aaron J. Cooper**[1], **John Svaren**[1,4]

[1]Waisman Center, University of Wisconsin-Madison, Madison, WI 53705, USA

[2]Cellular and Molecular Pathology Graduate Program, University of Wisconsin-Madison, Madison, WI 53705, USA

[3]Comparative Biomedical Sciences Graduate Program, University of Wisconsin-Madison, Madison, WI 53705, USA

[4]Department Of Comparative Biosciences, School of Veterinary Medicine, University of Wisconsin-Madison, Madison, WI 53705, USA

Abstract

Schwann cell programming during myelination involves transcriptional networks that activate gene expression but also repress genes that are active in neural crest/embryonic differentiation of Schwann cells. We previously found that a Schwann cell-specific deletion of the EED subunit of the Polycomb Repressive Complex (PRC2) led to inappropriate activation of many such genes. Moreover, some of these genes become re-activated in the pro-regenerative response of Schwann cells to nerve injury, and we found premature activation of the nerve injury program in a Schwann cell-specific knockout of *Eed*. Polycomb-associated histone modifications include H3K27 trimethylation formed by PRC2 and H2AK119 monoubiquitination (H2AK119ub1), deposited by Polycomb repressive complex 1 (PRC1). We recently found dynamic regulation of H2AK119ub1 in Schwann cell genes after injury. Therefore, we hypothesized that H2AK119 deubiquitination modulates the dynamic polycomb repression of genes involved in Schwann cell maturation. To determine the role of H2AK119 deubiquitination, we generated a Schwann cell-specific knockout of the H2AK119 deubiquitinase *Bap1 (BRCA1-associated protein)*. We found that loss of *Bap1* causes tomacula formation, decreased axon diameters and eventual loss of myelinated axons. The gene expression changes are accompanied by redistribution of H2AK119ub1 and H3K27me3 modifications to extragenic sites throughout the genome. BAP1 interacts with OGT in the PR-DUB complex, and our data suggest that the PR-DUB complex plays a multifunctional role in repression of the injury program. Overall, our results indicate *Bap1* is required to restrict the spread of polycomb-associated histone modifications in Schwann cells and to promote myelin homeostasis in peripheral nerve.

john.svaren@wisc.edu .

Conflict of interest disclosure: The authors declare there is no conflict of interest.

Ethics approval statement: All procedures described here were conducted in compliance with the Institutional Animal Care and Use Committee at the University of Wisconsin.

Graphical Abstract

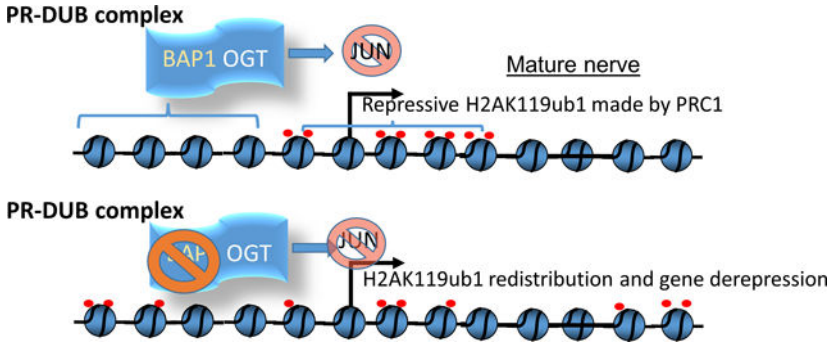

Keywords

Polycomb; deubiquitinase; histone; Schwann; nerve; injury

INTRODUCTION

Schwann cells play an important role in the stability, integrity, and function of the peripheral nervous system. In their terminally differentiated state, the myelin formed by Schwann cells enables saltatory conduction (1), and most cases of inherited neuropathy are caused by impaired Schwann cell function (2–4). Several studies have identified molecular determinants of a homeostatic phase upon myelin maturation, and several mouse mutants of neuropathy-associated genes have demonstrated progressive myelin deformations in adult nerve that eventually impact peripheral nerve function (5–13). Loss of myelin homeostasis can be prompted by alterations in key signaling pathways involved in neuregulin regulation, and also has been observed when epigenetic regulators are disrupted.

In previous studies, we tested the role of the Polycomb Repressive Complex 2 (PRC2), which forms repressive histone H3K27 trimethylation (H3K27me3), by creating a Schwann cell-specific knockout of the EED subunit of PRC2. We observed disruptions in myelin stability with a progressive hypermyelination of small caliber axons (14). Moreover, gene expression analysis revealed that EED had a role in maintaining repression of a significant proportion of the injury program that is normally activated only after peripheral nerve injury (14–16). The injury-induced reprogramming of mature Schwann cells allows transformation to pro-regenerative cells that support growth and survival of axons, clear myelin debris by autophagy/phagocytic responses, and form elongated Bungner bands to pave the way for nerve regeneration, before eventually myelinating any regenerated axons (17). Several transcription factors (e.g. c-JUN) are important activators of injury response genes (17–20). In addition, activation of the injury program was associated with reduction of repressive H3K27me3 on these injury genes (14, 15). Overall, these studies indicated that Polycomb repression was important to suppress the injury program in mature Schwann cells (16). In addition, this provides additional evidence that the homeostatic phase of myelination depends upon repression of JUN and the injury program (21, 22).

Polycomb repression is established by coordinate actions of PRC2 and PRC1, which catalyzes monoubiquitination of histone H2A (H2AK119ub1) through RING1A/B subunits (23). The canonical forms of PRC1 complexes are epigenetic readers of histone H3K27me3 formed by PRC2, leading to further repression through histone H2A ubiquitination and chromatin compaction (24). Accordingly, H2AK119ub1 is often associated with H3K27me3, and we found that H2AK119ub1 also decreases upon activation of polycomb-repressed injury genes (25). While PRC1-mediated repression was originally thought to be secondary to PRC2-dependent H3K27me3, there can be independent regulation of PRC1 complexes to establish H2AK119ub1 that triggers H3K27 methylation (23, 26, 27). Therefore, regulation of H2AK119ub1 can play a coequal or even primary role in establishing and maintaining polycomb repression.

The activity of the PRC1 and PRC2 complexes is opposed by epigenetic eraser proteins that can remove polycomb-associated histone modifications, such as the JMJD3/KDM6B demethylase for H3K27, and the BAP1 deubiquitinase for H2AK119 (28). We have previously tested the role of H3K27 demethylases in Schwann cell gene regulation. The Schwann cell-specific knockout of *Jmjd3/Kdm6b* and *Utx/Kdm6a* had little effect on Schwann cell development, other than some modest perturbations in PRC2-regulated genes. In addition, nerve injury responses in Schwann cells were temporally delayed but ultimately little affected at later stages of nerve injury (25).

We therefore decided to determine the role of the BAP1 deubiquitinase in Schwann cells. BAP1 is part of the PR-DUB (Polycomb Repressive-Deubiquitinase) complex, containing also O-Linked N-Acetylglucosamine (GlcNAc) Transferase (OGT) (29, 30). Based on the loss of H2AK119ub1 on injury-induced genes (25), we originally hypothesized that BAP1 may regulate polycomb repression of injury genes. Accordingly, we created a Schwann cell-specific deletion of the H2AK119 deubiquitinase, BAP1 (31). Loss of BAP1 led to impaired myelin homeostasis with tomacula and premature activation of the injury program, suggesting that writers and erasers of polycomb repression play mutually reinforcing roles in gene regulation and myelin homeostasis.

METHODS

Mouse Colony.

Animal experiments were performed according to protocols approved by the University of Wisconsin, Madison. *Bap1* floxed mice [Jackson Laboratories 031874] were maintained on the C57BL/6 genetic background and mated to mP0TOTA-Cre (*Mpz*-cre) (32). The *Bap1*tm1c(EUCOMM)Hmgu mouse strain carries a floxed (conditional) allele of *Bap1*, which is referred to as *Bap1* fl/fl. Derivation of the strain is described at http://www.informatics.jax.org/strain/MGI:6149727. Specifically, loxP sites flank exons 6–12 of the *Bap1* gene. We thank EUCOMM (European Conditional Mouse Mutagenesis Program) for making this strain available. the *Bap1* fl/fl and *Bap1* fl/fl/Mpz-cre genotypes are referred to as control and *Bap1* cKO, respectively. Genotyping employed primers for *Bap1*: TGGAAGGTAGTTGATTTTAGGC and GTGCACAGCCATCAGTGACT, and for the cre transgene: GAGTGATGAGGTTCGCAAGA-3’ and CTACACCAGAGACGGAAATC-3’

Morphometric quantification of myelination.

Freshly dissected sciatic nerves were immersion fixed in a solution of 2.5% glutaraldehyde, 2.0% paraformaldehyde in 0.1 M sodium phosphate buffer, pH 7.4, overnight at 4°. The nerves were then post-fixed in 1% osmium tetroxide in the same buffer for 2 h at room temperature. The nerves were dehydrated in a graded ethanol series, and then further dehydrated in propylene oxide and embedded in Epon resin. Ultrathin transverse sections were either contrasted with Reynolds lead citrate and 8% uranyl acetate in 50% ethanol or stained with toluidine blue. Images were obtained either with a Philips CM120 electron microscope with an AMT BioSprint side-mounted digital camera at the UW Medical School Electron Microscope Facility or with Nikon Ti2 microscopy. Quantification for g ratios was performed using NIS-Elements 4.0. Three mice per genotype were analyzed, and statistical analyses were evaluated using unpaired t-tests. Axons with myelination abnormalities (tomacula, in/outfolding) were not selected for g ratio quantitation.

Immunofluorescence.

Freshly dissected nerves were embedded in Tissue-Tek OCT compound (Sakura Finetek) and snap frozen with liquid nitrogen. Longitudinal or transverse cryostat sections (10 μm) were air-dried for 5 min and fixed in 4% paraformaldehyde for 10 min. The sections were then blocked in PBS containing 5% donkey serum/1% BSA/0.5% Triton-X 100 for 1 hr at room temperature. Primary antibody incubation was performed overnight at 4 ° in PBS containing 5% donkey serum/1% BSA/1% Triton-X 100 and secondary incubation was performed in PBS at room temperature for 1 hr. Hoechst 33342 (1:5,000 in PBS, Sigma) was applied to stain nuclei for 1 min. Three 4 min washes were performed in PBS after fixation and blocking, and in PBS containing 0.1% Tween20 after primary antibody incubation and nuclear staining. After coverslips were mounted using Fluoromount-G™ (SouthernBiotech), sections were examined on a Nikon A1R confocal and quantitated by both Columbus imaging software and manual curation.

For KI67 staining, tissue sections were blocked for 45 min with 2.5% donkey serum diluted in PBS, and then incubated with an anti-KI67 antibody, diluted 1:500 in blocking buffer, at 4° overnight. Tissue sections were washed with PBS-T (PBS with 0.05% Tween 20) three times, incubated with Alexa Fluor 488-conjugated secondary antibody (Invitrogen, A11008) at 25° for 45 min, and washed with PBS-T three times. Mounting medium containing DAPI (Electron Microscopy Sciences, 1798550) was applied, and tissue sections were imaged with a Nikon Eclipse Ti2 inverted microscope.

Western blot.

Freshly dissected nerves were snap frozen with liquid nitrogen and crushed. The nerves were then homogenized in lysis buffer (50 mM Tris–HCl at pH 6.8, 10% glycerol, 2% SDS, 10% β-mercaptoethanol, 50 mM NaF, 1 mM Na3VO4 and Protease Inhibitor Cocktail (Sigma, P8340) using a motorized pellet pestle. Cells in culture were homogenized in 3x lysis buffer. After a 15 min incubation in ice, lysates were boiled at 95 ° for 3 min and centrifuged at 4 ° for 15 min. Subsequently, supernatants were collected and subjected to SDS-PAGE. After transfer to polyvinylidene fluoride membrane, proteins were blocked in TBST containing 5% nonfat dry milk for 1 hr at room temperature. Primary and Secondary

antibody incubations were performed in TBST containing 5% BSA (Sigma, A7906) at 4 ° for overnight and at room temperature for 1 hr, respectively. Three 5 min-washes were performed in TBST after the incubations. The membranes were scanned and quantitated with the Odyssey Infrared Imaging System (Li-Cor Biosciences). Antibodies are listed in Table 1.

Quantitative RT-PCR.

RNA was isolated from sciatic nerves using the Trizol/chloroform RNA extraction protocol following purification with RNA Clean and Concentrator kit (Zymo). To prepare cDNA, 0.5–1 μg of total RNA was used from each sample. qRT-PCR and data analysis were performed as described previously (33). qPCR was performed in duplicate per sample. Primers for *Bap1* expression were: CTGGGCTCTCGTTGAACTACTCA and CCTCATCAGGGCCCTTCAC.

RNA seq.

Using control and *Bap1* cKO mice at 8 weeks of age (n=6/group), RNA was purified from sciatic nerves, and 1000 ng total RNA was sent to Genewiz (South Plainfield, NJ) for library preparation after PolyA selection and Illumina sequencing (Illumina HiSeq 2×150bp). Reads were aligned to GRCm38/mm10 genome using the STAR aligner (34). Data were analyzed using DESeq2 (35) to determine differentially regulated genes between wild type and *Bap1* KO mice (p-value < .05). RNA-seq data are deposited in NCBI GEO under accession number GSE197149.

Chromatin Immunoprecipitation.

Six freshly dissected mouse sciatic nerves per condition (*Bap1* fl/fl/Mpz-cre and *Bap1* fl/fl) were minced in 1% formaldehyde for 10min then quenched for 10 min with 0.125M glycine. Samples were incubated in LB1 for 10min, washed with LB2, then bead-homogenized using the Next Advance Bullet Blender for 5min with speed 12 (33). Samples were centrifuged to pull down nuclei-containing pellet. Pellet was resuspended in LB3 containing 0.1% SDS. Samples were sonicated via Bioruptor (Diagenode) on high for 2×15min cycles (30sec on/off). Sonicated chromatin was incubated with 5ug of target antibody. A 50 ul aliquot of Dynabead Protein G slurry was used to pull down the protein-antibody complex. A 10% aliquot of remaining chromatin was saved for input analysis. Immunoprecipitations were washed three times in RIPA buffer and then eluted at 65 °C in reverse cross-linking buffer (50 mM Tris, 10 mM EDTA, 1% SDS). ChIP-DNA was purified using the Cell Signaling DNA Purification Kit (CST #14209S). Antibodies used are in Table 1. Sample libraries were prepared from ChIP DNA, and respective inputs, using the Illumina TruSeq ChIP Sample Preparation Kit at the UW Biotechnology Center DNA Sequencing Facility. After sequencing on the Illumina Novaseq 6000, FastQ files were generated by bcl2fastq v2.20.0.422. H2AK119ub1 and H3K27me3 reads were mapped to the reference genome mm10 using Bowtie2. BAM files were filtered using the NGSUtils suite for mapped and properly paired reads. Peak tracks were generated using MACS2 callpeak relative to an input file. Bedgraph files were generated using the genome coverage tool in the bedtools suite. The data have been deposited in NCBI GEO GSE211544.

Bioinformatic Analysis.

The ChIP-seq data sets from mouse and similar data sets (GSE159265) of H2AK119ub1 in rat peripheral nerve (25) were used to create the heat maps for the deregulated genes. The data matrix for each heatmap and read density plots were generated using the EAseq suite (36) from filtered bam files based on ChIP-seq data sets and then clustered and visualized. Called peak annotations were created using ChIPSeeker (37). The gene ontology enrichment analyses were conducted with PANTHER and GSEA software to identify the enriched biological processes based on respective upregulated and downregulated lists of *Bap1* cKO genes. (38). For comparative analysis in transcriptomes, the statistical significance for the overlap between potential gene lists was tested at Nemaotes bioinformatic tools which utilizes the Fisher's Exact Test.

RESULTS

Conditional inactivation of *Bap1* in Schwann cells

To test the role of BAP1 in regulating Schwann cell development and maturation, we developed a Schwann cell specific conditional knockout (cKO) of *Bap1* using the *Mpz*-cre driver, which is active in embryonic Schwann cell development at E13.5-14.5 (32). The loxP sites surround exons 6–12 of *Bap1* including part of the catalytic UCH domain (Figure 1A) (39). The deletion results in a frameshift 3' of the deletion, leading to loss of the C-terminal sequence. The mouse knockout was validated by quantitative RT-PCR analysis of sciatic nerve cDNA using primers located in exons 7/8 in the deleted region, showing loss of *Bap1* expression in the conditional knockout (Figure 1A,B). The decrement in *Bap1* expression is consistent with the proportion of Schwann cells found in sciatic nerve. We also further confirmed the loss of BAP1 protein through immunostaining with an antibody targeting an epitope in the C-terminus of BAP1. Coexpression of BAP1 and SOX10, a marker of Schwann cells (40), was absent in the knockout whereas there are cells positive for such markers in control samples (Figure 1C, triangles).

Myelin abnormalities in the *Bap1* knockout

Mice with a Schwann cell-specific knockout of *Bap1* were overtly normal with no evident motor impairment after weaning. To determine if *Bap1* loss affects Schwann cell morphology, we performed toluidine blue staining of semi-thin sections to analyze the nerve ultrastructure (Figure 2A). At 6 weeks, the sciatic nerves of mutant mice were examined and many axons were observed to contain tomacula, and myelin infolding/outfolding (Figure 2B,C). *Bap1* cKO mice have a significantly greater prevalence of abnormal myelination compared to control (Figure 2C). Myelin thickness was assessed using the g-ratio, which is the axon diameter divided by outer diameter of myelin sheath (33). The overall g-ratio was not significantly different in the Bap1 cKO (Figure 2D). A binned analysis also showed no significant change in g ratios in any size range (not shown). However, the distribution of axon diameters was skewed with a notable deficit of the higher caliber axons (>4 micron) and an elevated number of smaller diameter axons (Figure 2E). The average median axon diameter for control was 2.97 microns (n=3), compared to 2.5 for the Bap1 cKO ($p=0.03$, 1-tailed t-test). We separately tested the overall distribution of axons in control vs. Bap1

cKO using the Mann-Whitney test, which yields a highly significant change in distribution ($p<10^{-14}$), although the effect size is small.

We also assessed femoral motor nerve at 4 months. While there was a clear thinning of myelin around large diameter axons (Figure 3), there was significant hypermyelination of smaller diameter axons (Figure 3C). The overall g ratio was reduced (0.62 in Bap1 cKO vs. 0.71 in control, n=4, p<0.0005, t-test). As seen in sciatic nerve, the distribution of axon diameters was shifted to an even greater degree, with the median diameter being reduced to 3.7 microns in the Bap1 cKO compared to 6.85 in the control (p<0.0005). Additionally, numerous amyelinated axons were observed in the *Bap1* cKO, which are rarely observed in wild type nerves. Quantitation of total myelinated axons in femoral motor nerve showed a reduction in *Bap1* cKO mice/nerves compared to control (avg. 337 vs 506, n=4, p<0.0005).

Derepression of injury genes in the BAP1 knockout

Given the myelin defects observed in the *Bap1* cKO, RNA-seq of sciatic nerve was used to compare *Bap1* cKO nerves and controls (n=6) at ~6 weeks of age. As shown in the volcano plot, there were widespread changes in gene expression (Figure 4A), and we identified 2446 upregulated and 2788 downregulated genes (p<0.05, FDR corrected, Supplementary Table 1). Gene Set Enrichment Analysis (Figure 4B) indicated that cholesterol and sterol biosynthesis and pathways are downregulated, whereas ribosome/polysome pathway genes are elevated by the loss of BAP1. The RNA-seq analysis did not suggest any increase in other cell populations such as macrophages. An independent gene ontology analysis via PANTHER (Supplementary Figure 1) revealed categories of upregulated genes associated with proliferation and gliogenesis (38). Enriched categories for downregulated genes included processes of Schwann cell differentiation and lipid synthesis (Supplementary Figure 1). The increase in cell cycle-associated genes revealed by RNA-seq suggested that there may be changes in proliferation. While there are normally very few proliferative cells in mature nerve, we did find an apparent increase in KI-67-positive cells in the Bap1 cKO (Supplementary Figure 4).

For further analysis, we used a >2-fold cutoff, yielding 708 upregulated genes and 604 downregulated genes in the *Bap1* cKO (Supplementary Table 2). Many of the downregulated genes were already expressed at relatively low levels in control and then repressed further in the *Bap1* cKO, but the downregulated Schwann cell genes include β-tubulin 4a (*Tubb4a*), Contactin 1 (*Cntn1*), Claudin 11 (*Cldn11*), Dual specificity phosphatase 26 (*Dusp26*), fatty acid elongase (*Elovl4*), and *Hoxb2*. Hox (homeobox) genes are commonly regulated by Polycomb repression. (16). In the downregulated dataset, there was modest downregulation of several myelin genes with *Mbp* being the most significant. Other genes are consistent with the ontology analysis that indicates downregulation of lipid biosynthetic genes.

Polycomb repression typically represses expression of transcription factors of other cell lineages (41–43). Schwann cells and oligodendrocytes share the ability to myelinate axons, but their regulatory networks are quite distinct (44) and two oligodendrocyte-specific transcription factors (*Myrf* and *Nkx6.2*) are induced in the *Bap1* cKO, along with MYRF target genes in oligodendrocytes (*Dct, Adamts4, Mog, Omg, Klk6, Ptgds, Rab33a*) (45, 46). Since MYRF is regulated by SOX10 (44), this would suggest that BAP1 is required to

prevent inappropriate expression of MYRF and oligodendrocyte gene networks in Schwann cells.

Polycomb-associated histone modifications in BAP1-regulated genes

To determine if BAP1 regulates polycomb histone modifications in Schwann cells, we also measured the levels of H2AK119ub1 by Western blot of sciatic nerve of the *Bap1* conditional knockout and found significantly increased levels of both histone marks (Figure 5A,B). Elevated H2AK119ub1 is consistent with the loss of H2A deubiquitinase activity, and increased levels of H3K27me3 likely reflects that PRC1 activity can stimulate H3K27me3 deposition by PRC2 (27, 47, 48).

Other studies have determined that BAP1 regulates the distribution of polycomb histone modifications in studies of cultured cells (49, 50)., but there has been limited analysis of BAP1 function in specific cell types in vivo. We then determined the genomic distribution of H2AK119ub1 and H3K27me3 in the control and *Bap1* conditional knockout mice, as we had done previously in rat sciatic nerve (14–16, 25). Peak calling for H2AK119ub1 in the control sample identified >35,000 peaks, and the heat maps over these peaks showed a decreased read density in the *Bap1* cKO (Figure 5C). In contrast, peak calling in the *Bap1 cKO* sample identified a much larger number (>60,000 peaks) of H2AK119ub1 occupied sites (Figure 5D). The increased number of peaks is reflected by the apparent increase of H2AK119ub1 read density at many of these sites in the Bap1 cKO compared to control. Therefore, BAP1 loss leads to a profound redistribution of the H2AK119ub1 modification from normal sites to an enlarged set of novel sites. Further analysis of read distribution in a binned analysis confirmed that the normal sites of H2AK119ub1 deposition were diminished in the *Bap1* cKO, but there was a redistribution of reads to the expanded peak set in the *Bap1* cKO (Supplementary Figure 2)

Changes in H2AK119ub1 can affect H3K27me3 deposition by PRC2 (27, 47, 48). A similar analysis of H3K27me3 (Figure 6A) showed that control peaks (12325) are diminished in the *Bap1* cKO, but peak calling in the cKO sample indicates sites that H3K27me3 becomes redistributed to other genomic locations in the *Bap1* cKO, resulting in a similar increase in the total number of H3K27me3 peaks (19308). The shift of H3K27me3 reads to an expanded peak set in the *Bap1* cKO was confirmed by distribution plot analysis (Supplementary Figure 3).

We wanted to determine if deregulated genes in the Bap1 cKO from the RNA-seq analysis were associated with polycomb repression, and more than a third of the upregulated genes are associated with H3K27me3 and/or H2AK119ub1 peaks. Specifically, at least 216 upregulated genes in the *Bap1* cKO are associated with both or either of histone marks, which includes many key nerve injury genes (e.g. *Shh, Gdnf*, and *Runx2*) which had been found to be regulated by *Eed* (15, 16, 25). In addition, 187 downregulated genes in the *Bap1* cKO are also associated with H2AK119ub1 and/or H3K27me3, suggesting that the redistribution of H2AK119ub1 may strengthen polycomb repression of some genes in the *Bap1* knockout.

BAP1 regulation of nerve injury genes.

Within the upregulated dataset, we observed several significant nerve injury genes that were prematurely activated in our analysis of PRC2 function in the *Eed* cKO (16), including *Shh, Gdnf, Fgf5, Hmga2, Vgf, and Igfbp2*. Upregulated genes include growth factors (*Neuregulin 1 and Betacellulin*) (51), cytokines (*Cxcl10*), and transcription factors (*Tfap2a, Runx2*, and *Pou3f1*) (14, 33, 52). Since our previous studies had indicated that loss of EED led to upregulation of a significant proportion of the nerve injury program in Schwann cells (14–16), we focused on the overlap between the nerve injury genes and the polycomb histone marks: H3K27me3 and H2AK119ub1 (Figure 7A). Our previous RNA-seq studies identified 1855 injury genes that are >2-fold induced in sciatic nerve (1 and 7 d post-transection gene, Supplementary Table 3) (16). Using the called peaks from the histone modification analysis, we found that around 844 out of 1855 injury-induced genes are associated with either or both histone marks. 327 genes have promoter-proximal peaks for both H2AK119ub1 and H3K27me3. There are 182 injury genes with called peaks for H2AK119ub1 alone and 335 genes with H3K27me3 alone.

Focusing on the set of 844 injury genes associated with H3K27me3 and/or H2AK119ub1, a significant set are affected by BAP1 cKO. At least 70 *Bap1*-dependent upregulated genes that are induced by nerve injury are also associated with either or both histone marks. Several of them are prominent nerve injury genes including *Gdnf, Igfbp2, Pou3f1, Fgf5, Shh, Runx2,* and *Hmga2* (53, 54). In contrast, only 10 injury-induced genes associated with either or both histone marks are downregulated in the *Bap1* cKO (Figure 7B). Figure 7C shows the peaks of H2AK119ub1 in the *Gdnf* and *Nrg1* type 1 promoters, which are diminished in the *Bap1* cKO.

Comparison of the roles of BAP1 and OGT

BAP1 interacts with OGT as subunits of the PR-DUB complex (29, 30), and a Schwann-cell specific *Ogt* KO mouse model exhibited deficient remyelination after injury that was traced to the premature activation of JUN in uninjured nerve (21, 55). The *Ogt* mutant mouse exhibited a significant number of tomacula and thinner myelination of larger caliber axons, with eventual loss of myelinated axons, which is similar in several respects to the *Bap1* cKO. We determined if a common PR-DUB target gene set could be defined by comparative analysis of genes regulated by OGT and BAP1, we compared the RNA seq data of the *Bap1* cKO to the published RNA-seq analysis of the *Ogt c*KO (21). Out of 1298 upregulated genes with significant p-values in *Ogt*-KO datasets (Supplementary Table 2), there are 153 matches with upregulated *Bap1* cKO genes and 54 matches with downregulated *Bap1* cKO genes (Figure 8C).

Interactions of polycomb-regulated genes with the JUN-regulated network of injury genes.

A significant proportion of dysregulated target genes in the *Ogt* cKO are unchanged in the *Bap1* cKO. An important feature of the *Ogt* knockout is the activation of JUN in uninjured nerve (21), as expression of JUN can drive demyelination (22). While JUN is a major regulator of nerve injury program in Schwann cell (20), JUN is normally not expressed at high levels prior to injury. It is possible that part of the induction of injury genes could be mediated by JUN, since there is a slight 1.7-fold induction of the *c-Jun* transcript in our

RNA-seq analysis of the *Bap1* knockout. Therefore, we examined the JUN by western blot but observed no significant difference in JUN expression between genotypes at 6 weeks of age (Figure 8A,B).

It is still possible that JUN activity is stimulated post-transcriptionally, and RNA-seq indicates that *Fos*, a component of AP-1, is upregulated 2.8-fold. Therefore, we compared the RNA seq profile of the BAP1 cKO to RNA-seq analysis of a mouse model with Schwann cell-specific JUN overexpression (22). Using this data set, there are only 11 common genes that are upregulated in both BAP1 cKO and the JUN overexpression model, such *as Shh, S100a4, Btc*, and *Cxcl10* (Supplementary Table 5). The overlap between upregulated *Bap1* cKO and c-JUN cKO genes is significant ($p < 2e\text{-}10$). While there is overlapping regulation of injury genes by JUN and polycomb repression, the evidence indicates that they also play independent roles since we do not see induction of the entire JUN target gene network in Schwann cells. Therefore, we conclude that BAP1's active role in regulating nerve injury genes is not mediated by JUN. There is also an overlap of JUN-regulated genes and those that were found to be deregulated in the EED cKO, but we also did not detect measurable induction of JUN in the EED cKO (16).

DISCUSSION

Since premature activation of the Schwann cell injury program has been shown to adversely impact the formation of stable myelin (21, 22), several mechanisms have been identified that repress injury genes in mature Schwann cells. One of these mechanisms, Polycomb repression, is regulated by diverse complexes that impinge on this type of regulation. In particular, there are multiple assemblies of PRC2 and PRC1 complexes that can play unique roles in establishing polycomb repression in different genes (28, 56). Our previous study of the *Eed* knockout in Schwann cells revealed roles in the regulation of myelin homeostasis and also in repression of the injury program (14–16). PRC2 regulation in Schwann cells has been tied to interactions with CTCF and the ACTL6A-containing BAF complex (57, 58) and loss of PRC2 regulation is a critical step in formation of malignant peripheral nerve sheath tumors in Neurofibromatosis (16, 59). However, PRC2 regulation is intertwined in several respects with PRC1, and we had found changes in PRC1-mediated H2A ubiquitination in Schwann cells after injury (25).

To understand how dynamics of H2AK119 ubiquitination affect polycomb repression in Schwann cells, we focused on the BAP1 deubiquitinase, which is a component of PR-DUB complex that also includes other subunits like OGT and ASXL1/2 (30, 60). Loss of BAP1 in Schwann cells causes an abnormal myelin morphology that is evident at six weeks. Specifically, there are increased levels of tomacula and abnormal myelin, and some large caliber axons have thinner myelin in the mutant mouse, although the overall g ratio is unaffected at this time point. Analysis of femoral motor nerve at 4 months showed a more severe phenotype, with a shift of axon distribution to smaller calibers with thicker myelin, accompanied by a reduction in the total number of myelinated axons. Overall, these phenotypes are similar to those seen in the Schwann cell-specific knockout of *Eed* (14), although somewhat more severe, indicating an important role of BAP1 in myelin homeostasis.

An RNA-seq analysis of sciatic nerve revealed significant changes in gene regulation. Importantly, we found that several key nerve injury genes are prematurely activated in *Bap1* cKO mice including *Shh, Gdnf, Runx2, Hmga2*, *Cdkn2a*, and *Fgf5,* which were also activated in the *Eed* ckO (16), but this analysis revealed a broader range of polycomb-repressed genes, many of which are associated with H2AK119 ubiquitination. The gene expression changes are similar in several respects with previous analysis of a Schwann cell knockout of OGT, which interacts with BAP1 in the PR-DUB complex. The Schwann cell-specific *Ogt*-cKO leads to elevated JUN activity, resulting in the premature activation of nerve injury genes and a significant degree of tomacula and thinner myelination of larger caliber axons. Specifically, OGT suppresses the nerve injury response by catalyzing O-glcnacylation of the JUN protein (21, 55), and one of the striking findings of the OGT analysis was that the failed regeneration after injury could be rescued by deletion of one allele of *Jun* (21).

Since BAP1 and OGT are part of the PR-DUB complex, it was possible that loss of *Bap1* could phenocopy the myelination defects seen in *Ogt*-KO (at 3 months), and the myelin defects showed some similarities as noted above. A comparison of the RNA-seq data sets revealed that 153 out of 708 upregulated genes in *Bap1* cKO overlaps with those of *Ogt*-KO genes suggesting that there is some level of functional overlap, but there are also quite significant differences in the transcriptomic effect of BAP1 loss. Some of these 153 genes are Schwann cell nerve injury genes, which could explain the abnormal myelination in *Bap1* cKO mouse model. However, *Jun* was only slightly elevated (1.7-fold) in the RNA-seq analysis. Moreover, we did not observe any change in JUN protein in the *Bap1* cKO. Using *Ogt*-KO RNA seq data (21), there were 11 matches out of 28 upregulated JUN target genes with *Bap1* cKO genes. Therefore, we conclude that BAP1 and OGT appear to play overlapping but functionally distinct roles within a multifunctional PR-DUB complex by maintaining polycomb repression of the nerve injury program and inhibiting JUN, respectively. These roles are mutually reinforcing since there is considerable overlap of JUN-regulated and polycomb-regulated genes in the nerve injury response (16). Accordingly, OGT is less tightly associated with BAP1 compared to other PR-DUB subunits and can participate in other complexes (29, 60).

Several of the deregulated genes could cause the myelination defects in *Bap1* mutant Schwann cells. One gene that was derepressed in both the *Eed* and *Bap1* cKO is IGF-binding protein 2 (*Igfbp2),* which was shown to increase PI3 kinase signaling (14). Another leading candidate is the *Neuregulin 1* type I (*Nrg1)* gene, since previous studies have found that efficient remyelination of injured nerves requires the de novo activation of type I NRG1 in denervated Schwann cells (61). We had found that H3K27me3 mediates repression of *Nrg1* and there is increased expression of the type I *Nrg1* transcript in the uninjured Eed cKO nerves (16). Our data also indicate the presence of H2AK119ub1 on the *Nrg1* type 1 promoter (Figure 7). A recent study showed that overexpression of NRG1 type 1 is responsible for hypermyelination of small caliber axons and the onion bulb pathology that has been observed in CMT1A neuropathy (62). Another potential mechanism could involve BAP1 regulation of the PTEN lipid phosphatase, since a Schwann cell-specific deletion of *Pten* caused hypermyelination (8, 63). It has been reported that BAP1 could repress *Pten* at the transcriptional and post-transcriptional levels (64, 65). However, *Pten* levels were not

elevated in our RNA-seq analysis and Western blot showed no change in PTEN protein levels (data not shown).

Since PRC1 and PRC2 regulation are connected at multiple levels, we compared the deregulated genes with those obtained in our previous RNA-seq profiling of a Schwann cell-specific deletion of *Eed* (16). Although we had speculated that deletion of *Bap1* could result in strengthened Polycomb repression, we observed derepression of many polycomb-regulated genes; 105 upregulated *Bap1*-KO genes are in common with those upregulated in the *Eed* conditional knockout (Supplementary Table 4). Additionally, there are 52 downregulated genes that are regulated by EED. It was unexpected that deletion of the BAP1 deubiquitinase as a polycomb modification eraser would have a similar phenotype and overlapping gene expression changes with inhibition of the PRC2 writer complex in the *Eed* cKO (14). Several cell culture studies have characterized the role of BAP1 and divergent results have been obtained. In some cases, loss of BAP1 leads to increased polycomb repression which is associated with increased levels of H2AK119ub1 (60, 66). In contrast, other studies have shown that loss of BAP1 leads to loss of polycomb repression (49, 50). This has been attributed to a function of BAP1 to safeguard transcriptionally silent genes by preventing accumulation of extragenic H2AK119 and H3K27me3 modifications that would titrate out polycomb repression if allowed to spread (49, 50). Accordingly, the Drosophila homolog of BAP1, calypso, was originally classified as a polycomb group gene (31). These mechanisms are highly relevant to the observed mutation of *BAP1* in several types of cancer since both gain- and loss-of-function models of polycomb repression can contribute to malignancy (49, 56, 66, 67). In our case, we found both increased levels of H2AK119ub1 and H3K27me3 in peripheral nerve, and also a larger number of called peaks for H2AK119ub1 and H3K27me3 in our ChIP-seq analysis of *Bap1* mutant nerve. Our study is unique in that we have analyzed the effect of *Bap1* on polycomb repression in post-mitotic Schwann cells in vivo compared to previous studies in cell culture models. However, based on the earlier studies (49, 50), our data are consistent with a model in which derepression of some polycomb-associated genes is due to inappropriate accumulation of H2AK119ub1 and H3K27me3 at new sites across the genome.

Numerous pro-regenerative genes in Schwann cells are repressed by both H2AK119ub1 and H3K27me3 and their basal expression can be virtually undetectable in intact, healthy peripheral nerve. Previous studies had suggested that removal of polycomb repression is required for induction of nerve injury genes such as *Shh*, and *Gdnf* (14–16). PRC2 is commonly known to work cooperatively with PRC1, but recent studies had indicated that PRC1-mediated repression can be mediated independently of PRC2 (28). Moreover, it has emerged that phenotypes of PRC1-related phenotypes are often more severe than PRC2 mutants (68), and the *Bap1* knockout phenotype is more severe than either the Eed or the Jmjd3/Utx knockouts in Schwann cells (25). Therefore, future experiments will be used to determine if deubiquitinase(s) play a role in regulation of injury genes in Schwann cells.

Supplementary Material

Refer to Web version on PubMed Central for supplementary material.

Acknowledgments:

The authors thank Randall Massey from the Electron Microscopy Facility for processing microscopy samples, and the University of Wisconsin Biotechnology Center DNA Sequencing Facility (Research Resource Identifier – RRID:SCR_017759) for providing for providing RNA library preparation, and sequencing services. We also thank Kaye Thomas for assistance in image analysis.

Funding:

This work was supported by the National Institutes of Health: R01 NS100510 to JS, and by a core grant to the Waisman Center from the Eunice Kennedy Shriver National Institute of Child Health and Human Development (P50 HD105353).

Data availability:

The data that support the findings of this study are openly available in NCBI Gene Expression Omnibus at https://www.ncbi.nlm.nih.gov/geo/, accession number GSE197149 and GSE211544.

References

1. Mirsky R, andJessen KR (1996) Schwann cell development, differentiation and myelination Curr Opin Neurobiol 6, 89–96 [PubMed: 8794046]
2. Nelis E, Haites N, Van Broeckhoven C (1999) Mutations in the peripheral myelin genes and associated genes in inherited peripheral neuropathies Hum Mutat 13, 11–28 [PubMed: 9888385]
3. Saporta MA, andShy ME (2013) Inherited peripheral neuropathies Neurol Clin 31, 597–619 10.1016/j.ncl.2013.01.009 [PubMed: 23642725]
4. Stassart RM, Möbius W, Nave KA, andEdgar JM (2018) The Axon-Myelin Unit in Development and Degenerative Disease Front Neurosci 12, 467 10.3389/fnins.2018.00467 [PubMed: 30050403]
5. Rosenberg LH, Cattin AL, Fontana X, Harford-Wright E, Burden JJ, White IJ et al. (2018) HDAC3 Regulates the Transition to the Homeostatic Myelinating Schwann Cell State Cell Rep 25, 2755–2765.e2755 10.1016/j.celrep.2018.11.045 [PubMed: 30517863]
6. Beirowski B, Wong KM, Babetto E, andMilbrandt J (2017) mTORC1 promotes proliferation of immature Schwann cells and myelin growth of differentiated Schwann cells Proc Natl Acad Sci U S A 114, E4261–E4270 10.1073/pnas.1620761114 [PubMed: 28484008]
7. Domènech-Estévez E, Baloui H, Meng X, Zhang Y, Deinhardt K, Dupree JL et al. (2016) Akt Regulates Axon Wrapping and Myelin Sheath Thickness in the PNS J Neurosci 36, 4506–4521 10.1523/JNEUROSCI.3521-15.2016
8. Cotter L, Ozçelik M, Jacob C, Pereira JA, Locher V, Baumann R et al. (2010) Dlg1-PTEN interaction regulates myelin thickness to prevent damaging peripheral nerve overmyelination Science 328, 1415–1418 10.1126/science.1187735 [PubMed: 20448149]
9. Goebbels S, Oltrogge JH, Wolfer S, Wieser GL, Nientiedt T, Pieper A et al. (2012) Genetic disruption of Pten in a novel mouse model of tomaculous neuropathy EMBO Mol Med 4, 486–499 10.1002/emmm.201200227
10. Bolino A, Piguet F, Alberizzi V, Pellegatta M, Rivellini C, Guerrero-Valero M et al. (2016) Niacin-mediated Tace activation ameliorates CMT neuropathies with focal hypermyelination EMBO Mol Med 8, 1438–1454 10.15252/emmm.201606349
11. Golan N, Kartvelishvily E, Spiegel I, Salomon D, Sabanay H, Rechav K et al. (2013) Genetic deletion of Cadm4 results in myelin abnormalities resembling Charcot-Marie-Tooth neuropathy J Neurosci 33, 10950–10961 10.1523/JNEUROSCI.0571-13.2013 [PubMed: 23825401]
12. He X, Zhang L, Queme LF, Liu X, Lu A, Waclaw RR et al. (2018) A histone deacetylase 3-dependent pathway delimits peripheral myelin growth and functional regeneration Nat Med 24, 338–351 10.1038/nm.4483 [PubMed: 29431744]

13. Pantera H, Hu B, Moiseev D, Dunham C, Rashid J, Moran JJ et al. (2020) Pmp22 super-enhancer deletion causes tomacula formation and conduction block in peripheral nerves Hum Mol Genet 29, 1689–1699 10.1093/hmg/ddaa082 [PubMed: 32356557]

14. Ma KH, Hung HA, Srinivasan R, Xie H, Orkin SH, andSvaren J (2015) Regulation of Peripheral Nerve Myelin Maintenance by Gene Repression through Polycomb Repressive Complex 2 J Neurosci 35, 8640–8652 10.1523/JNEUROSCI.2257-14.2015 [PubMed: 26041929]

15. Ma KH, Hung HA, andSvaren J (2016) Epigenomic Regulation of Schwann Cell Reprogramming in Peripheral Nerve Injury J Neurosci 36, 9135–9147 10.1523/JNEUROSCI.1370-16.2016 [PubMed: 27581455]

16. Ma KH, Duong P, Moran JJ, Junaidi N, andSvaren J (2018) Polycomb repression regulates Schwann cell proliferation and axon regeneration after nerve injury Glia 66, 2487–2502 10.1002/glia.23500 [PubMed: 30306639]

17. Jessen KR, andMirsky R (2019) The Success and Failure of the Schwann Cell Response to Nerve Injury Front Cell Neurosci 13, 33 10.3389/fncel.2019.00033 [PubMed: 30804758]

18. Ramesh R, Manurung Y, Ma KH, Blakely T, Won S, Wyatt E et al. (2022) JUN Regulation of Injury-induced Enhancers in Schwann Cells bioRxiv 2022.01.31.478565, 10.1101/2022.01.31.478565

19. Wagstaff LJ, Gomez-Sanchez JA, Fazal SV, Otto GW., Kilpatrick AM. et al. (2021) Failures of nerve regeneration caused by aging or chronic denervation are rescued by restoring Schwann cell c-Jun Elife 10, e62232 10.7554/eLife.62232 [PubMed: 33475496]

20. Arthur-Farraj PJ, Latouche M, Wilton DK, Quintes S, Chabrol E, Banerjee A et al. (2012) c-Jun reprograms Schwann cells of injured nerves to generate a repair cell essential for regeneration Neuron 75, 633–647 10.1016/j.neuron.2012.06.021 [PubMed: 22920255]

21. Kim S, Maynard JC, Strickland A, Burlingame AL, andMilbrandt J (2018) Schwann cell O-GlcNAcylation promotes peripheral nerve remyelination via attenuation of the AP-1 transcription factor JUN Proc Natl Acad Sci U S A 115, 8019–8024 10.1073/pnas.1805538115 [PubMed: 30012597]

22. Fazal SV, Gomez-Sanchez JA, Wagstaff LJ, Musner N, Otto G, Janz M et al. (2017) Graded elevation of c-Jun in Schwann cells in vivo: gene dosage determines effects on development, re-myelination, tumorigenesis and hypomyelination J Neurosci 37, 12297–12313 10.1523/JNEUROSCI.0986-17.2017 [PubMed: 29109239]

23. Blackledge NP, Rose NR, andKlose RJ (2015) Targeting Polycomb systems to regulate gene expression: modifications to a complex story Nat Rev Mol Cell Biol 16, 643–649 10.1038/nrm4067 [PubMed: 26420232]

24. Tamburri S, Lavarone E, Fernández-Pérez D, Conway E, Zanotti M, Manganaro D et al. (2020) Histone H2AK119 Mono-Ubiquitination Is Essential for Polycomb-Mediated Transcriptional Repression Mol Cell 77, 840–856.e845 10.1016/j.molcel.2019.11.021 [PubMed: 31883952]

25. Duong P, Ma KH, Ramesh R, Moran JJ, Won S, andSvaren J (2021) H3K27 demethylases are dispensable for activation of Polycomb-regulated injury response genes in peripheral nerve J Biol Chem 297, 100852 10.1016/j.jbc.2021.100852 [PubMed: 34090875]

26. Li G, Margueron R, Ku M, Chambon P, Bernstein BE, andReinberg D (2010) Jarid2 and PRC2, partners in regulating gene expression Genes Dev 24, 368–380 10.1101/gad.1886410 [PubMed: 20123894]

27. Cooper S, Grijzenhout A, Underwood E, Ancelin K, Zhang T, Nesterova TB et al. (2016) Jarid2 binds mono-ubiquitylated H2A lysine 119 to mediate crosstalk between Polycomb complexes PRC1 and PRC2 Nat Commun 7, 13661 10.1038/ncomms13661 [PubMed: 27892467]

28. Blackledge NP, andKlose RJ (2021) The molecular principles of gene regulation by Polycomb repressive complexes Nat Rev Mol Cell Biol 22, 815–833 10.1038/s41580-021-00398-y [PubMed: 34400841]

29. Hauri S, Comoglio F, Seimiya M, Gerstung M, Glatter T, Hansen K et al. (2016) A High-Density Map for Navigating the Human Polycomb Complexome Cell Rep 17, 583–595 10.1016/j.celrep.2016.08.096 [PubMed: 27705803]

30. Dey A, Seshasayee D, Noubade R, French DM, Liu J, Chaurushiya MS et al. (2012) Loss of the tumor suppressor BAP1 causes myeloid transformation Science 337, 1541–1546 10.1126/science.1221711 [PubMed: 22878500]

31. Scheuermann JC, de Ayala Alonso AG, Oktaba K, Ly-Hartig N, McGinty RK, Fraterman S et al. (2010) Histone H2A deubiquitinase activity of the Polycomb repressive complex PR-DUB Nature 465, 243–247 10.1038/nature08966 [PubMed: 20436459]

32. Feltri ML, D'Antonio M, Previtali S, Fasolini M, Messing A, andWrabetz L (1999) P0-Cre transgenic mice for inactivation of adhesion molecules in Schwann cells Ann N Y Acad Sci 883, 116–123

33. Hung HA, Sun G, Keles S, andSvaren J (2015) Dynamic regulation of Schwann cell enhancers after peripheral nerve injury J Biol Chem 290, 6937–6950 10.1074/jbc.M114.622878 [PubMed: 25614629]

34. Dobin A, Davis CA, Schlesinger F, Drenkow J, Zaleski C, Jha S et al. (2013) STAR: ultrafast universal RNA-seq aligner Bioinformatics 29, 15–21 10.1093/bioinformatics/bts635 [PubMed: 23104886]

35. Anders S, McCarthy DJ, Chen Y, Okoniewski M, Smyth GK, Huber W et al. (2013) Count-based differential expression analysis of RNA sequencing data using R and Bioconductor Nat Protoc 8, 1765–1786 10.1038/nprot.2013.099 [PubMed: 23975260]

36. Lerdrup M, Johansen JV, Agrawal-Singh S, andHansen K (2016) An interactive environment for agile analysis and visualization of ChIP-sequencing data Nat Struct Mol Biol 23, 349–357 10.1038/nsmb.3180 [PubMed: 26926434]

37. Yu G, Wang LG, andHe QY (2015) ChIPseeker: an R/Bioconductor package for ChIP peak annotation, comparison and visualization Bioinformatics 31, 2382–2383 10.1093/bioinformatics/btv145 [PubMed: 25765347]

38. Mi H, Ebert D, Muruganujan A, Mills C, Albou LP, Mushayamaha T et al. (2021) PANTHER version 16: a revised family classification, tree-based classification tool, enhancer regions and extensive API Nucleic Acids Res 49, D394–D403 10.1093/nar/gkaa1106 [PubMed: 33290554]

39. Lin YH, Liang Y, Wang H, Tung LT, Förster M, Subramani PG et al. (2021) Regulation of B Lymphocyte Development by Histone H2A Deubiquitinase BAP1 Front Immunol 12, 626418 10.3389/fimmu.2021.626418 [PubMed: 33912157]

40. Britsch S, Goerich DE, Riethmacher D, Peirano RI, Rossner M, Nave KA et al. (2001) The transcription factor Sox10 is a key regulator of peripheral glial development Genes Dev 15, 66–78 [PubMed: 11156606]

41. Boyer LA, Plath K, Zeitlinger J, Brambrink T, Medeiros LA, Lee TI et al. (2006) Polycomb complexes repress developmental regulators in murine embryonic stem cells Nature 441, 349–353 10.1038/nature04733 [PubMed: 16625203]

42. Lee TI, Jenner RG, Boyer LA, Guenther MG, Levine SS, Kumar RM et al. (2006) Control of developmental regulators by Polycomb in human embryonic stem cells Cell 125, 301–313 10.1016/j.cell.2006.02.043 [PubMed: 16630818]

43. Bracken AP, Dietrich N, Pasini D, Hansen KH, andHelin K (2006) Genome-wide mapping of Polycomb target genes unravels their roles in cell fate transitions Genes Dev 20, 1123–1136 10.1101/gad.381706 [PubMed: 16618801]

44. Lopez-Anido C, Sun G, Koenning M, Srinivasan R, Hung HA, Emery B et al. (2015) Differential Sox10 genomic occupancy in myelinating glia Glia 63, 1897–1914 10.1002/glia.22855 [PubMed: 25974668]

45. Emery B, Agalliu D, Cahoy JD, Watkins TA, Dugas JC, Mulinyawe SB et al. (2009) Myelin gene regulatory factor is a critical transcriptional regulator required for CNS myelination. Cell 138, 172–185 S0092–8674(09)00456–5 [pii] 10.1016/j.cell.2009.04.031 [PubMed: 19596243]

46. Bujalka H, Koenning M, Jackson S, Perreau VM, Pope B, Hay CM et al. (2013) MYRF Is a Membrane-Associated Transcription Factor That Autoproteolytically Cleaves to Directly Activate Myelin Genes Plos Biology 11, 10.1371/journal.pbio.1001625

47. Tavares L, Dimitrova E, Oxley D, Webster J, Poot R, Demmers J et al. (2012) RYBP-PRC1 complexes mediate H2A ubiquitylation at polycomb target sites independently of PRC2 and H3K27me3 Cell 148, 664–678 10.1016/j.cell.2011.12.029 [PubMed: 22325148]

48. Kalb R, Latwiel S, Baymaz HI, Jansen PW, Müller CW, Vermeulen M et al. (2014) Histone H2A monoubiquitination promotes histone H3 methylation in Polycomb repression Nat Struct Mol Biol 21, 569–571 10.1038/nsmb.2833 [PubMed: 24837194]
49. Conway E, Rossi F, Fernandez-Perez D, Ponzo E, Ferrari KJ, Zanotti M et al. (2021) BAP1 enhances Polycomb repression by counteracting widespread H2AK119ub1 deposition and chromatin condensation Mol Cell 81, 3526–3541.e3528 10.1016/j.molcel.2021.06.020 [PubMed: 34186021]
50. Fursova NA, Turberfield AH, Blackledge NP, Findlater EL, Lastuvkova A, Huseyin MK et al. (2021) BAP1 constrains pervasive H2AK119ub1 to control the transcriptional potential of the genome Genes Dev 35, 749–770 10.1101/gad.347005.120 [PubMed: 33888563]
51. Newbern J, andBirchmeier C (2010) Nrg1/ErbB signaling networks in Schwann cell development and myelination Semin Cell Dev Biol 21, 922–928 10.1016/j.semcdb.2010.08.008 [PubMed: 20832498]
52. Quintes S, Brinkmann BG, Ebert M, Fröb F, Kungl T, Arlt FA et al. (2016) Zeb2 is essential for Schwann cell differentiation, myelination and nerve repair Nat Neurosci 19, 1050–1059 10.1038/nn.4321 [PubMed: 27294512]
53. Boyd JG, andGordon T (2003) Glial cell line-derived neurotrophic factor and brain-derived neurotrophic factor sustain the axonal regeneration of chronically axotomized motoneurons in vivo Exp Neurol 183, 610–619 [PubMed: 14552902]
54. Hashimoto M, Ishii K, Nakamura Y, Watabe K, Kohsaka S, andAkazawa C (2008) Neuroprotective effect of sonic hedgehog up-regulated in Schwann cells following sciatic nerve injury J Neurochem 107, 918–927 10.1111/j.1471-4159.2008.05666.x [PubMed: 18786173]
55. Kim S, Maynard JC, Sasaki Y, Strickland A, Sherman DL, Brophy PJ et al. (2016) Schwann Cell O-GlcNAc Glycosylation Is Required for Myelin Maintenance and Axon Integrity J Neurosci 36, 9633–9646 10.1523/JNEUROSCI.1235-16.2016 [PubMed: 27629714]
56. Tamburri S, Conway E, andPasini D (2021) Polycomb-dependent histone H2A ubiquitination links developmental disorders with cancer Trends Genet 10.1016/j.tig.2021.07.011
57. Park HJ, Tsai E, Huang D, Weaver M, Frick L, Alcantara A et al. (2022) ACTL6a coordinates axonal caliber recognition and myelination in the peripheral nerve iScience 25, 104132 10.1016/j.isci.2022.104132 [PubMed: 35434551]
58. Wang J, Yang L, Zhao C, Wu LN, Xu L, Zhang F et al. (2020) CTCF-mediated chromatin looping in EGR2 regulation and SUZ12 recruitment critical for peripheral myelination and repair Nat Commun 11, 4133 10.1038/s41467-020-17955-2 [PubMed: 32807777]
59. Sohier P, Luscan A, Lloyd A, Ashelford K, Laurendeau I, Briand-Suleau A et al. (2017) Confirmation of mutation landscape of NF1-associated malignant peripheral nerve sheath tumors Genes Chromosomes Cancer 56, 421–426 10.1002/gcc.22446 [PubMed: 28124441]
60. Campagne A, Lee MK, Zielinski D, Michaud A, Le Corre S, Dingli F et al. (2019) BAP1 complex promotes transcription by opposing PRC1-mediated H2A ubiquitylation Nat Commun 10, 348 10.1038/s41467-018-08255-x [PubMed: 30664650]
61. Stassart RM, Fledrich R, Velanac V, Brinkmann BG, Schwab MH, Meijer D et al. (2013) A role for Schwann cell-derived neuregulin-1 in remyelination Nat Neurosci 16, 48–54 10.1038/nn.3281 [PubMed: 23222914]
62. Fledrich R, Akkermann D, Schütza V, Abdelaal TA, Hermes D, Schäffner E et al. (2019) NRG1 type I dependent autoparacrine stimulation of Schwann cells in onion bulbs of peripheral neuropathies Nat Commun 10, 1467 10.1038/s41467-019-09385-6 [PubMed: 30931926]
63. Goebbels S, Oltrogge JH, Kemper R, Heilmann I, Bormuth I, Wolfer S et al. (2010) Elevated phosphatidylinositol 3,4,5-trisphosphate in glia triggers cell-autonomous membrane wrapping and myelination J Neurosci 30, 8953–8964 10.1523/JNEUROSCI.0219-10.2010 [PubMed: 20592216]
64. Cao L, Xia X, Kong Y, Jia F, Yuan B, Li R et al. (2020) Deregulation of tumor suppressive ASXL1-PTEN/AKT axis in myeloid malignancies J Mol Cell Biol 12, 688–699 10.1093/jmcb/mjaa011 [PubMed: 32236560]
65. Chen X, Huang A, Wang Y, Chen F, Hu B, Zhang X et al. (2021) BRCA1-associated protein 1 serves as a tumor suppressor in hepatocellular carcinoma by deubiquitinating and stabilizing PTEN Am J Cancer Res 11, 2044–2061 [PubMed: 34094668]

66. LaFave LM, Béguelin W, Koche R, Teater M, Spitzer B, Chramiec A et al. (2015) Loss of BAP1 function leads to EZH2-dependent transformation Nat Med 21, 1344–1349 10.1038/nm.3947 [PubMed: 26437366]

67. Daou S, Barbour H, Ahmed O, Masclef L, Baril C, Sen Nkwe N et al. (2018) Monoubiquitination of ASXLs controls the deubiquitinase activity of the tumor suppressor BAP1 Nat Commun 9, 4385 10.1038/s41467-018-06854-2 [PubMed: 30349006]

68. Cohen I, Bar C, andEzhkova E (2020) Activity of PRC1 and Histone H2AK119 Monoubiquitination: Revising Popular Misconceptions Bioessays 42, e1900192 10.1002/bies.201900192 [PubMed: 32196702]

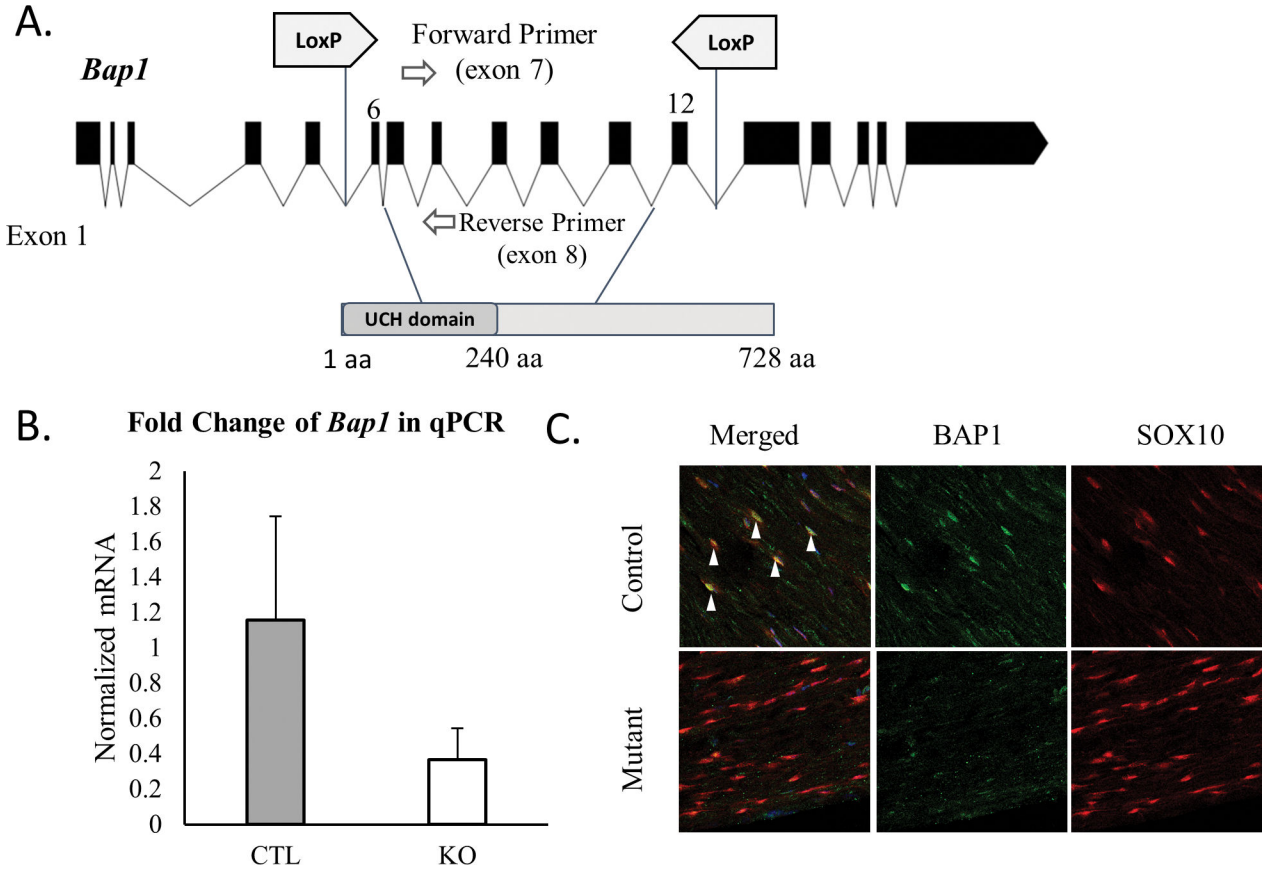

Figure 1. Schwann-cell specific knockout of *Bap1*.

A. The *Bap1* conditional allele contains loxP sites flanking exons 6–12, which encode part of the catalytic domain. **B. The** qRT-PCR analysis of RNA extracted from the control and BAP1 cKO sciatic nerves was performed using primers within the excised regions. $P<0.05$ unpaired t-test, n=3/group. **C.** Immunofluorescence analysis of the longitudinal sections from the wildtype and BAP1 cKO sciatic nerves was performed using the indicated antibodies. n=3 for control and n=3 for cKO. Error bars indicate standard deviation.

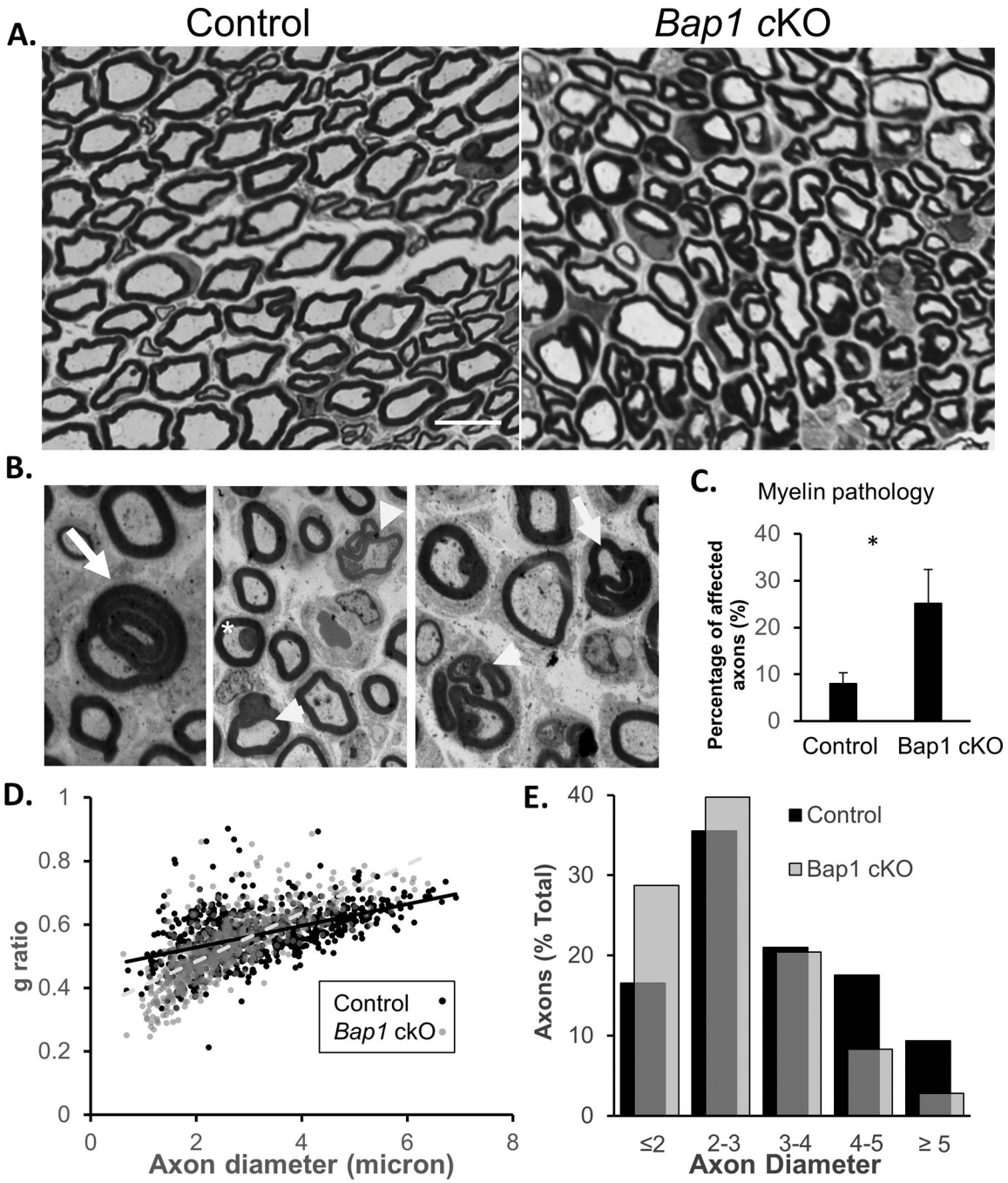

Figure 2. Myelin morphology in the *Bap1* cKO.

A. Electron micrographs of the sciatic nerves at 6 weeks of *Bap1* cKO mice and littermate controls. **B**. The highlighted fibers display abnormal morphologies, including tomacula (arrow), and outfolding (arrowhead) and infolding (asterisk). **C.** Quantitation shows increased occurrence of abnormal myelin profiles (including tomacula and in/outfolding) in the *Bap1* cKO compared to the control ($p<0.05$, unpaired t-test, n=3/group). **D.** For g-ratio analysis, the axon and outer diameters of myelinated fibers were measured on randomly selected fibers per genotype. The overall g ratios were not significantly different between

the Bap1 cKO and control. **E.** The bar graph shows the distribution of axon diameters in control vs. *Bap1* cKO. The average median diameter for control was 2.97 microns (n=3), compared to 2.5 for the Bap1 cKO (p=0.03, 1-tailed t-test). A Mann-Whitney test of the overall distribution of axons in control vs. Bap1 cKO yields a highly significant change in distribution ($p<10^{-14}$). Data: n=3 per genotype, 717 WT vs 745 cKO axons were counted.

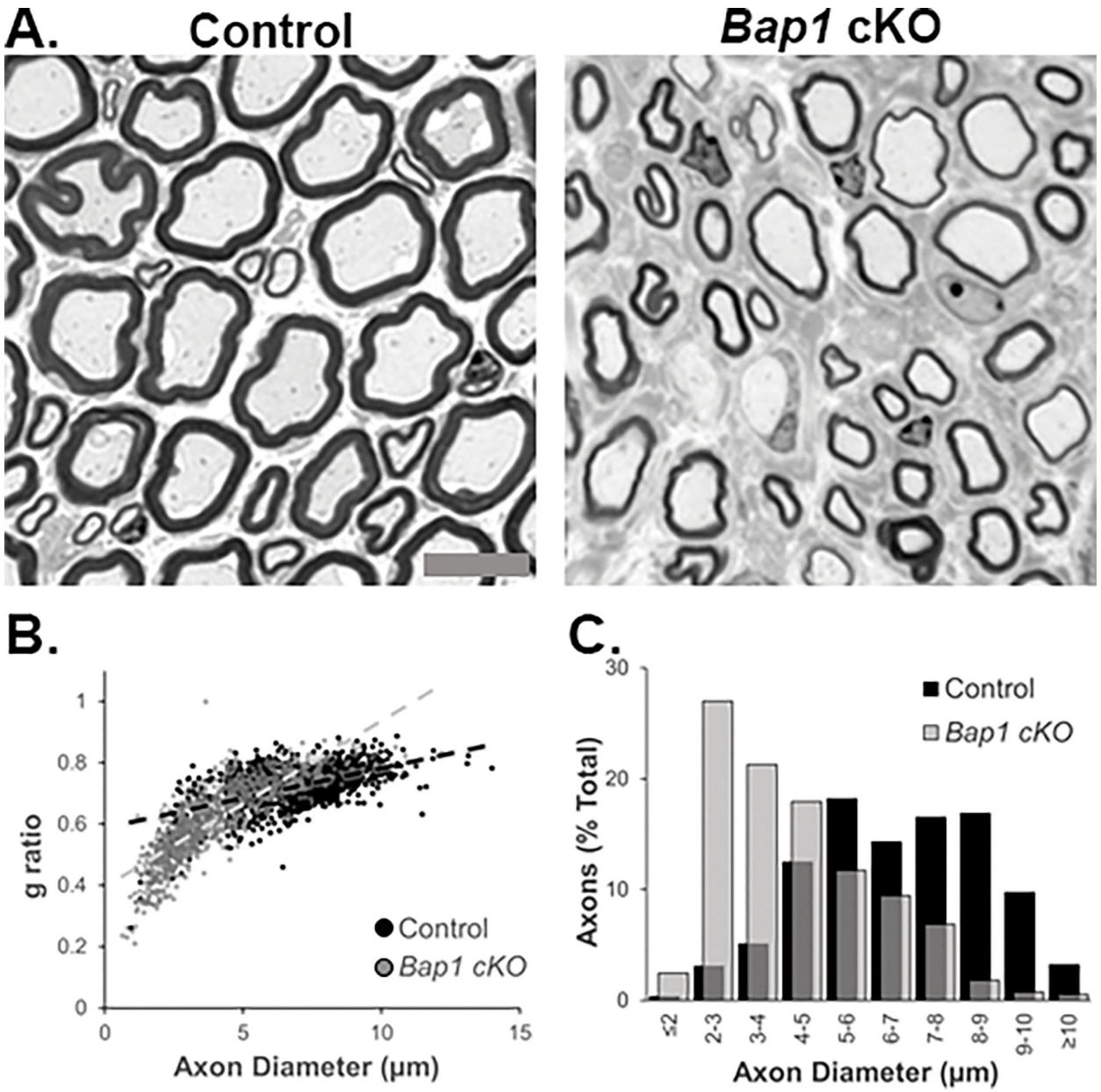

Figure 3. Myelin morphology in the femoral motor nerve.

A. Toluidine blue-stained semithin sections of femoral motor nerve of 4 month old *Bap1* cKO mice and littermate controls. **B.** For g-ratio analysis, axon and myelinated fiber diameters were measured on all femoral motor nerve axons per genotype. The overall g ratio was reduced (0.62 in Bap1 cKO vs. 0.71 in control, n=4, $p<0.0005$, t-test). **C.** The bar graph shows the distribution of axon diameters in control vs. *Bap1* cKO. The median axon diameter is reduced to 3.7 microns in the Bap1 cKO compared to 6.85 in the control ($p<0.0005$). The total number of myelinated axons is reduced in Bap1 cKO mice/nerves compared to control (avg. 337 vs 506 per nerve, n=4, $p<0.0005$).

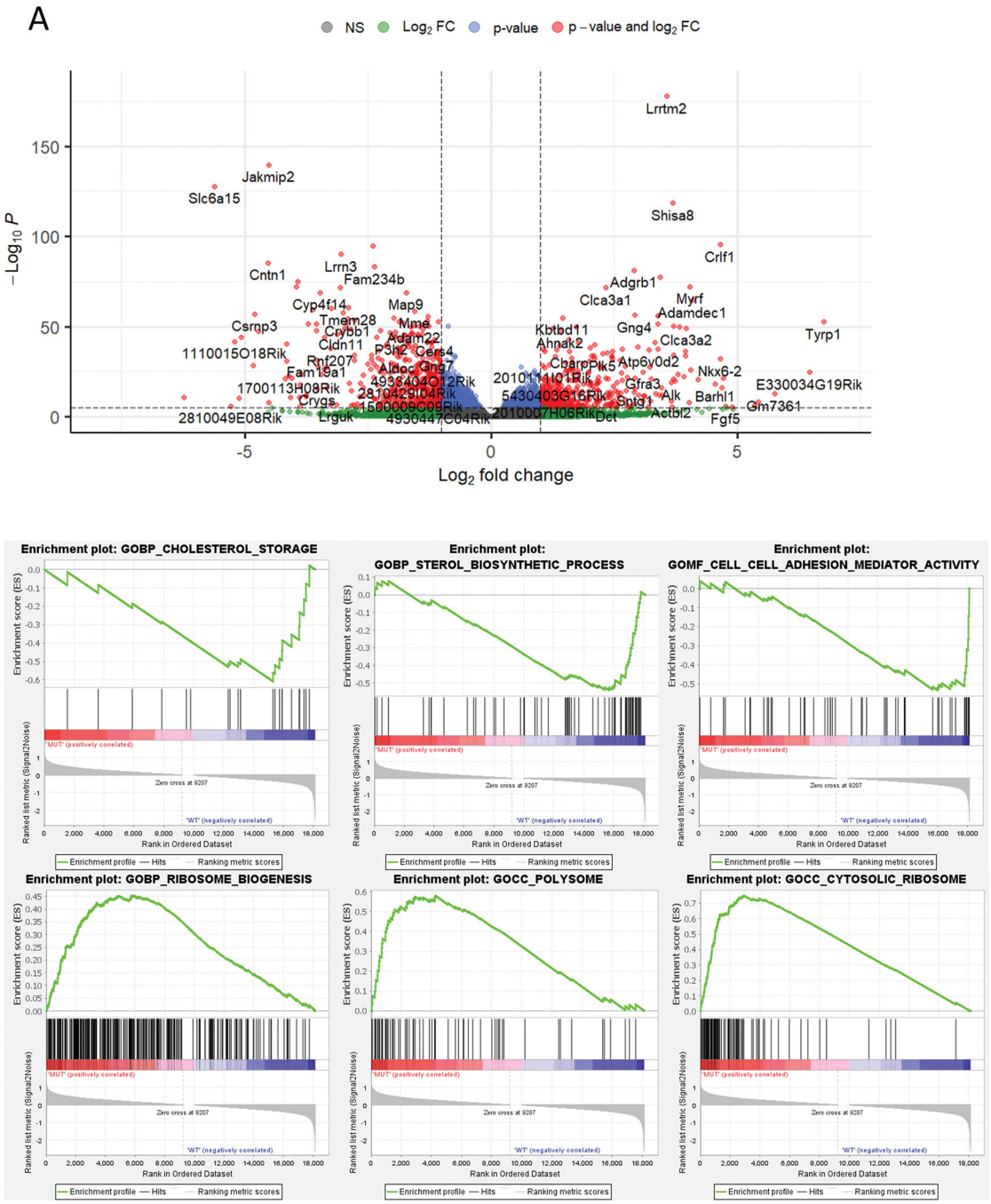

Figure 4. RNA-seq analysis of *Bap1* cKO mice.

A. RNA-seq analysis was performed in 6 week old *Bap1* cKO and littermate controls (n=6/genotype). Volcano plots indicate increased and decreased genes in the *Bap1* cKO relative to control after filtering for >2-fold change and <0.05 p value. **B**. GSEA enrichment plots summarize some of the major biological and cellular processes that are affected in the *Bap1* cKO.

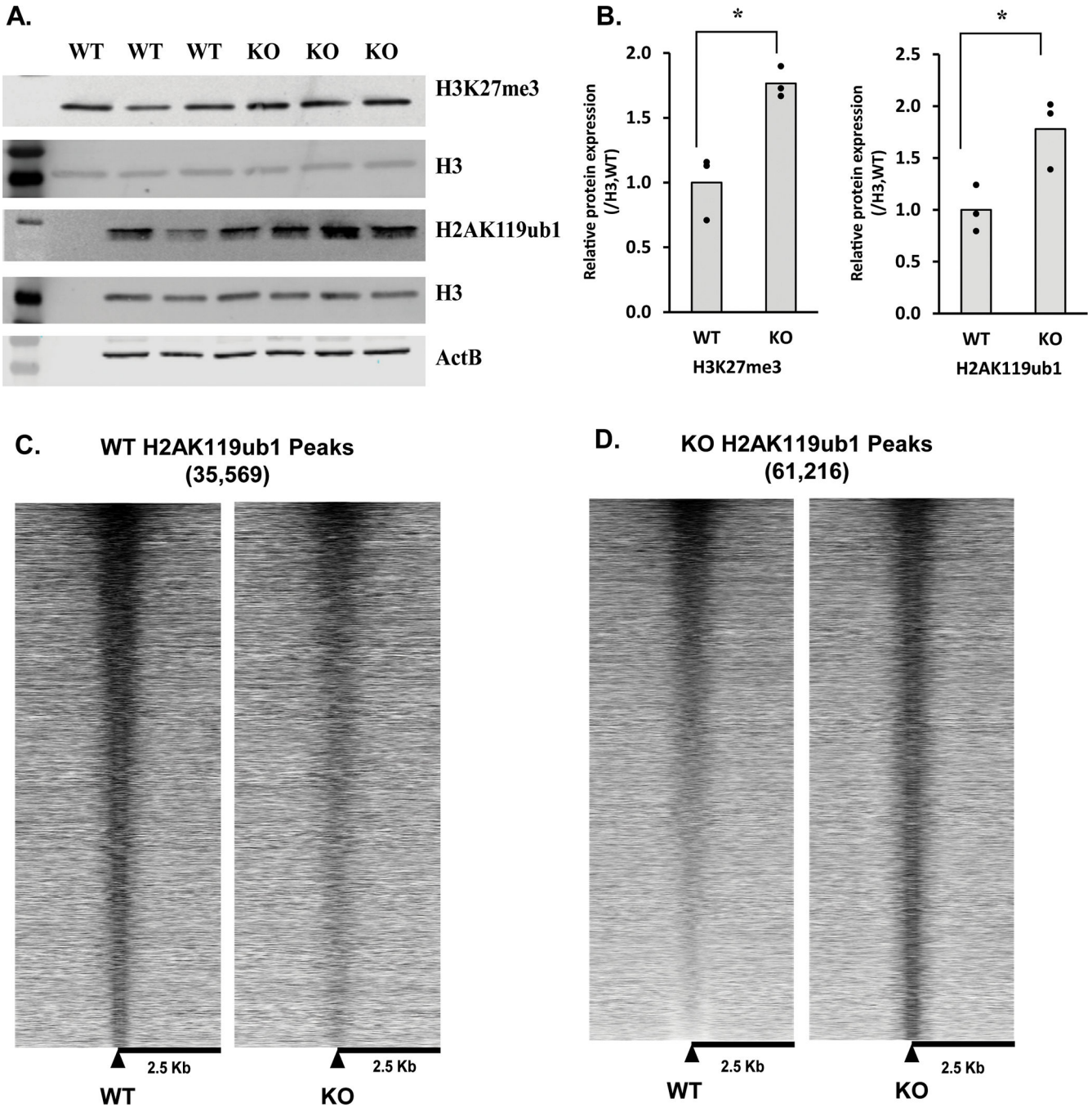

Figure 5. Loss of *Bap1* causes redistribution of H2AK119ub1.

A. Western blot analysis of lysates from the sciatic nerves in control and mutant was performed using the indicated antibodies. **B.** The quantification of western blot results indicating the relative expression of the histone modifications normalized to total histone H3. Individual data points are shown ($p<0.05$, n=3, t-test). **C.** ChIP-seq analysis of H2AK119ub1 was performed in control and *Bap1* cKO sciatic nerve, and heatmaps of control and knockout show density of H2AK119ub1 reads centered on the control peak locations. The heatmaps indicate decreased read density of H2AK119ub1 at these sites in

the *Bap1* cKO. **D.** The ChIP-seq analysis of H2AK119ub1 in *Bap1* cKO nerve shows an increased number of peaks compared to the control. Using the expanded *Bap1* cKO peak set, the heatmaps of wildtype and knockout H2AK119ub1 reads centered on knockout peaks show accumulation of H2AK119ub1 at many of the *Bap1* cKO peaks compared to control.

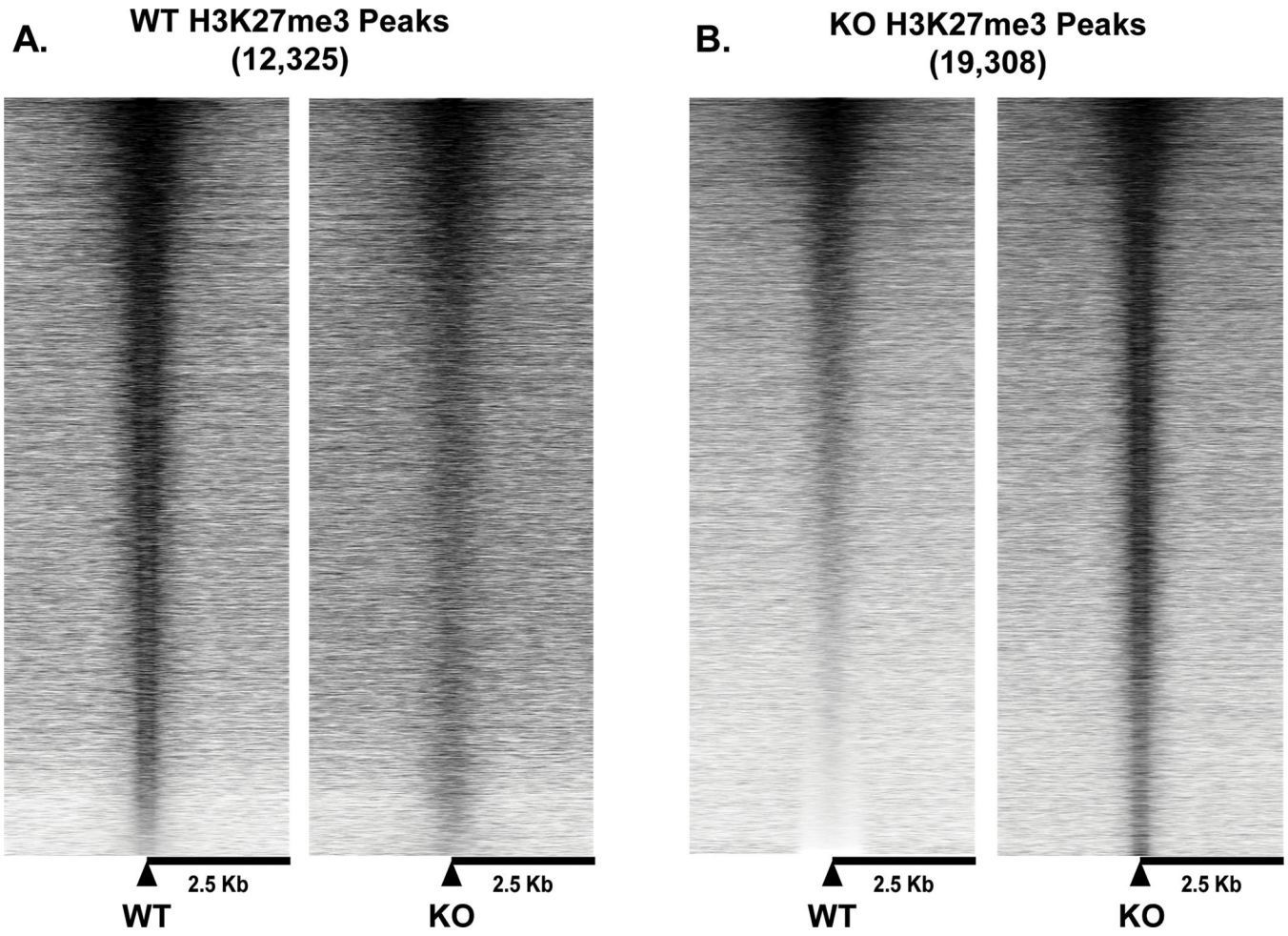

Figure 6. The H3K27me3 histone modification is redistributed similar to H2AK119ub1 in the *Bap1* knockout.

A. ChIP-seq analysis of H3K27me3 was performed in control and *Bap1* cKO sciatic nerve, and heatmaps of wildtype and knockout H3K27me3 reads centered on wildtype peaks show the loss of H3K27me3 at these sites in *Bap1* cKO nerve. **B.** Peak calling in the *Bap1* cKO ChIP-seq analysis of H3K27me3 identified an increased number of peaks compared to control. Heatmaps of wildtype and knockout H3K27me3 reads centered on *Bap1* cKO peaks show increased read density of H3K27me3 in the expanded peak set compared to control.

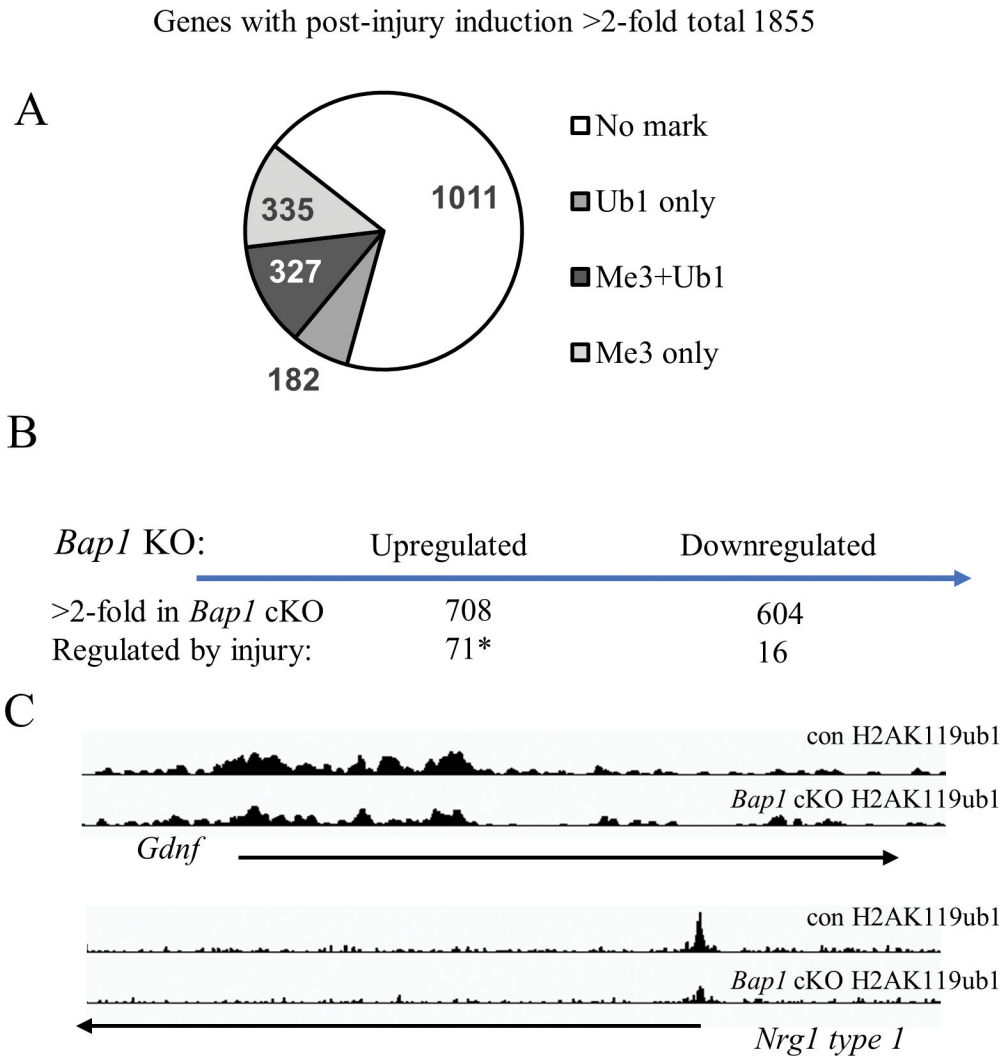

Figure 7. Association of nerve injury genes with polycomb-associated histone modifications.

A. The pie chart indicates injury-induced genes in sciatic nerve as determined by RNA-seq analysis. The proportion of these genes associated with either or both polycomb-associated histone modifications (H2AK119ub1 and/or H3K27me3) is indicated by shading. **B.** The overlap of injury-induced genes and those genes with altered regulation in the *Bap1* cKO is shown. **C.** Profiles of H2AK119ub1 from the ChIP-seq analysis of control and *Bap1* cKO nerve show localization at the transcription start sites for two injury-induced genes: *Gdnf* and *Nrg1* type 1.

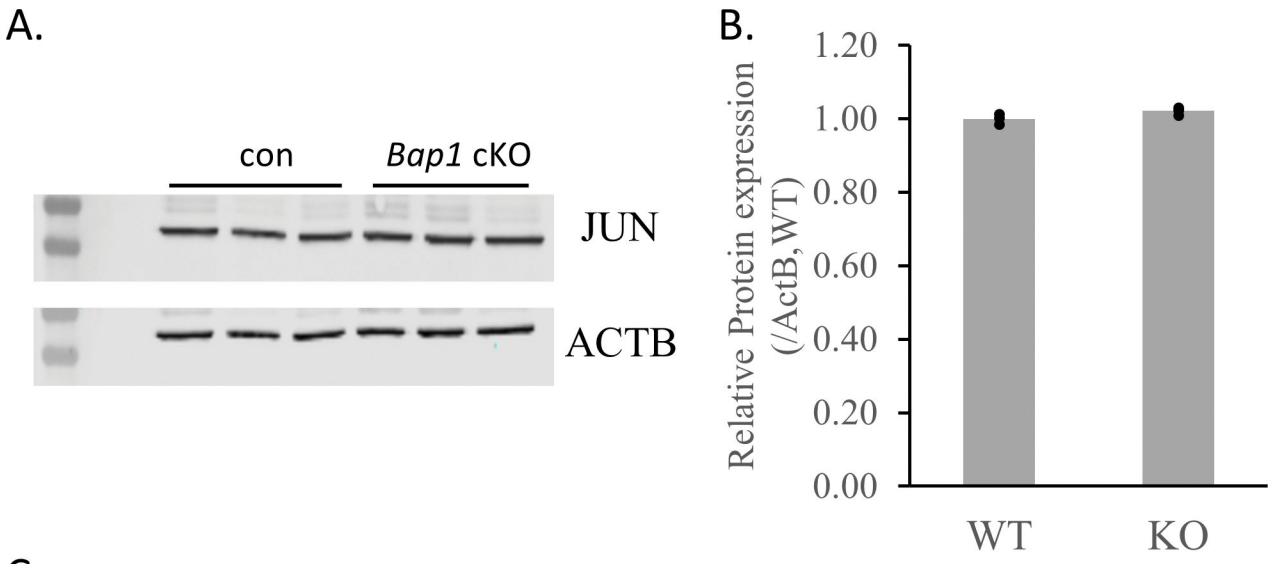

C.

Bap1 cKO:	Upregulated	Downregulated
> 2-fold in cKO	708	604
Regulated by OGT:	153*	54*

Figure 8. c-JUN is not affected in the *Bap1* knockout.

A. Western blot analysis of lysates from the sciatic nerves in control and mutant was performed using the indicated antibodies. **B.** Quantification of c-JUN protein expression is shown relative to ACTB in bar graph. Data: n=3/group Individual data points are shown. **C.** The overlap of Bap1-regulated and OGT-regulated genes is shown.

Table 1.

List of Antibodies Used.

Antibodies	Catalog number	Company
SOX10	AF2864	R & D Systems
Ki67	Ab16667	Abcam
BAP1	13271	Cell Signaling Technology
ACTB	#AC004	Abclonal
IgG	12–370	Millipore
H2AK119ub1	8240	Cell Signaling Technology
H3K27me3	AM39155	Active Motif
H3	14269	Cell Signaling Technology
c-JUN	9165	Cell Signaling Technology
PTEN	9188	Cell Signaling Technology